Ice response to an underwater body moving in a frozen channel

Konstantin Shishmarev[a,*], Tatyana Khabakhpasheva[b], Alexander Korobkin[c]

[a] *Altai State University, Barnaul, Russia*
[b] *Lavrentyev Institute of Hydrodynamics, Novosibirsk, Russia*
[c] *School of Mathematics, University of East Anglia, Norwich, UK*

Abstract

Strains in the ice cover of a frozen channel, which are caused by a body moving under the ice at a constant speed along the channel, are studied. The channel is of rectangular cross section, the fluid in the channel is inviscid and incompressible. The ice cover is modeled by a thin viscoelastic plate clamped to the channel walls. The underwater body is modeled by a three-dimensional dipole. The intensity of the dipole is related to the speed and size of the underwater body. The problem is considered within the linear theory of hydroelasticity. For small deflections of the ice cover the velocity potential of the dipole in the channel is obtained by the method of images without account for ice deflection in the leading order. The problem of a dipole moving in the channel with rigid walls provides the hydrodynamic pressure on the upper boundary of the channel, which corresponds to the ice cover. This pressure distribution does not depend on the deflection of the ice cover in the leading approximation. The deflections of ice and the strains in the ice cover are independent of time in the coordinate system moving together with the dipole. The problem is solved numerically using the Fourier transform along the channel, the method of normal modes across the channel, and the truncation method for resulting infinite systems of linear equations. It was revealed that the strains in the ice strongly depend on the speed of the dipole with respect to the critical speeds of the hydroelastic waves propagating along the frozen channel. The width of the channel matters even it is much larger than the characteristic length of the ice cover.

Keywords: Elastic plate, Dipole, Ice defections and strains, Underwater body

1. Introduction

The problems of the ice cover response to applied external loads have been well studied for an unbounded ice cover [1] and for a semi-infinite ice cover clamped to a vertical wall [2]. The external loads were modelled by ether a point pressure or a smooth localized pressure distribution moving with a constant speed along the ice cover. The problems were studied within the linear theory of hydroelasticity. The ice deflections and strain distributions in the ice cover were determined. A main practical goal of those studies was to answer the question whether the ice can be broken or not by an applied moving pressure and where this would happen, close to the load or at a distance from it.

The ice deflection and strains in the ice plate due to a localized external load moving along the channel were investigated in [3, 4]. The effect of the channel parameters and characteristics of the ice plate on the

*Corresponding author
Email address: shishmarev.k@mail.ru (Konstantin Shishmarev)

ice deflections and strain distribution in the ice cover were studied. A relevant problem of hydroelastic waves propagating along a frozen channel was studied in [5, 6] within the linear theory of hydroelasticity.

The tree-dimensional problem of ice deflection caused by a dipole moving horizontally in the fluid under the ice cover was studied in [7]. The fluid was unbounded horizontally and infinitely deep. The ice cover and fluid were initially at rest. The initial compression of the ice was taken into account. A dipole started to move instantly at a constant speed. The ice deflection was obtained using the Fourier transforms. It was shown that the ice deflection approaches a steady state for large times in the coordinate system moving together with the dipole. The speed of the dipole in [7] was below the critical speed, defined in [1], for the ice cover. The deflection was maximum just above the dipole with the ice plate deflecting down towards the dipole. The ice deflection quickly decayed with the distance from the dipole.

A similar problem in the two-dimensional formulation was studied in [8, 9]. The two-dimensional problem of a pulsating point source placed in an infinitely deep ice-covered fluid was investigated in [10]. The solution was obtained as a superposition of standing and traveling waves. The frequencies of both the standing and traveling waves were equal to the frequency of the source strength oscillation. The amplitudes and wavenumbers of the obtained hydroelastic waves were shown to be strongly depend on the thickness and elastic properties of the ice.

The two-dimensional problem of a cylinder moving with large amplitude oscillations in a deep fluid covered with ice was investigated in [11]. The problem was solved using multipole expansion method. The effects of both the ice properties and the parameters of the motion on the hydrodynamic force acting on the cylinder and the ice plate deflection were investigated. Linear and nonlinear boundary conditions were used. The nonlinearity was shown to be important for vertical motions of the body, where the distance from the body to the ice cover changes in time.

The motions of slender bodies in a fluid under an ice cover were studied in [12]. The ice cover was modelled as an infinite thin elastic plate. The fluid was of infinite depth. The slender body in a fluid was modelled by the source-sink system in the three-dimensional formulation. The distance of the body from the ice cover, the ice thickness and the size of the body affected the amplitudes of the generated hydroelastic waves. It was shown that the ice cover can be broken by the moving slender body for certain ranges of the parameters of the ice and the body velocity. The obtained theoretical results were compared with the experimental results for a submarine moving under a continuous ice plate. Motion of a single source under the ice was investigated in [13].

Small oscillations of a two-dimensional submerged body in a fluid partly covered with ice were studied by Sturova and Tkacheva [14, 15, 16] within the linear theory of hydroelasticity. In these studies, the upper boundary of the fluid consisted of either two semi-infinite intervals of free surfaces and a floating elastic plate or a finite interval of the free surface between two semi-infinite elastic plates of different thicknesses. The oscillating body was placed either under the ice or under the free surface. The problem was reduced to an integral equation for an unknown distribution of mass sources on the equilibrium position of the body surface. The amplitudes of the vertical displacements of both the free surface and elastic plates were determined. It was shown that the generated flow strongly depends on the position of the submerged body with respect to the elastic plates [15]. This analysis can be extended to the three-dimensional problems with oscillating submerged bodies.

The two-dimensional problem of hydroelastic wave interaction with a body submerged below an ice cover

with a crack was studied in [17]. The body was modelled by a circular cylinder within the multipole expansion method. The ice cover was modelled by a thin uniform elastic plate with the conditions of zero bending moment and zero shear force at the crack. The problem was solved using the boundary element method within the linearized potential theory. Similar problems including those with different numbers of cracks in the ice cover were investigated in [18].

In the present paper, the problem of ice deflection caused by an underwater body moving along a frozen channel is considered. This problem is approximately identical to the problem of a stationary body placed in a uniform current under the ice cover in a channel, if viscosity of the fluid is negligible. The moving body is modelled by a three-dimensional dipole of a constant strength. The dipole moving at a constant speed in an unbounded fluid generates the flow and the pressure corresponding to a rigid sphere moving at the same speed [19]. The radius of the sphere is related to the speed of the dipole and its strength. A dipole moving in a channel with rigid walls also represents approximately a rigid sphere if the dipole strength is so small that the corresponding sphere radius is much smaller than both the distance from the dipole to the walls of the channel and the depth of the channel. For a dipole moving relatively close to a wall, the shape of the corresponding rigid body is not spherical. This shape can be approximately determined. This fictitious body is inside the channel and does not touch the channel walls.

The velocity potential of a dipole placed in a rectangular channel with rigid walls is determined by the method of images. The potential of several dipoles is the superposition of the corresponding potentials of individual dipoles. A system of dipoles can be arranged in such a way that they accurately represent a body of a given shape. By using the known velocity potential and the unsteady Bernoulli equation, the hydrodynamic loads acting on the channel walls are determined. For a dipole of small strength, the linearized Bernoulli equation is used. This case corresponds to the motion of a small sphere along the channel covered with ice. The hydrodynamic loads on the ice cover caused by a moving underwater body are determined in the leading order without account for the ice deflection. The ice deflection is determined thereafter as the ice response to the loads caused by the moving body. Even for small deflections of the ice cover, the strains in the cover can be large enough to cause ice breaking. The Kelvin-Voigt model of viscoelastic ice plate is used in the present study to estimate the strains in the ice cover. In this model, hydroelastic waves decay with distance from the load due to the damping effect. The viscoelastic ice model is closer to reality than the elastic ice plate model without dampimg.

The problem formulation and three asymptotic models with small deflections of the ice cover are presented in Section 2. Only the model of a weak dipole is coupled. The problem within this approximate model is solved by using the Fourier transform and normal mode decomposition in Section 3. Numerical results are reported and discussed in Section 4. The conclusions are drawn in Section 5.

2. Formulation of the problem

The hydroelastic waves generated by an underwater body moving along a channel covered with ice are considered in the Cartesian coordinates x, y, z. The channel is of rectangular cross section and is infinitely long.

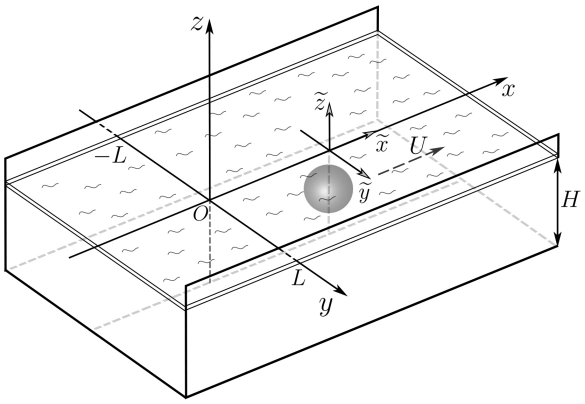

Рис. 1: The scheme of the problem with main notation.

The scheme of the problem is shown on the Figure 1. The ice cover is modelled as a viscoelastic plate [1],

$$Mw_{tt} + D\left(1 + \tau\frac{\partial}{\partial t}\right)\nabla_2^4 w = p(x, y, w(x, y, t), t) \qquad (-\infty < x < \infty,\ -L < y < L,\ z = w(x, y, t)), \tag{1}$$

where $w(x, y, t)$ is the deflection of the ice plate, $2L$ is the width of the channel, x is the coordinate along the channel, D is the rigidity coefficient, $M = \rho_i h_i$ is the mass of the ice plate per unit area, ρ_i is the ice density, h_i is the ice plate thickness, τ is the retardation time in the Kelvin-Voight model of viscoelastic ice plate [23], $\nabla_2^4 w = \partial^4 w/\partial x^4 + 2\partial^4 w/\partial x^2\partial y^2 + \partial^4 w/\partial y^4$ is the biharmonic operator, and $p(x, y, z, t)$ is the hydrodynamic pressure caused by both the moving body and deflection of the ice cover of the channel, z is the vertical coordinate. Here $z = -H$ corresponds to the bottom of the channel and $z = 0$ to the initial position of the interface between the water in the channel and the flat ice plate. The ice plate is frozen to the walls of the channel, which is modelled by the clamped conditions,

$$w = 0, \quad w_y = 0 \qquad (-\infty < x < \infty, \quad y = \pm L). \tag{2}$$

The water in the channel is modelled as an incompressible and inviscid fluid. The moving body is represented by a dipole. The flow caused by a moving dipole is potential and three-dimensional with the velocity potential $\varphi_{tot}(x, y, z, t)$. The hydrodynamic pressure is given by the nonlinear Bernoulli equation,

$$p(x, y, z, t) = -\rho_l\left(\frac{\partial\varphi_{tot}}{\partial t} + \frac{1}{2}|\nabla\varphi_{tot}|^2 + gz\right), \tag{3}$$

where ρ_l is the fluid density, and g is the gravitational acceleration. Initially, $t = 0$, the fluid and the ice plate are at rest,

$$\varphi_{tot} = 0, \qquad \varphi_{tot,t} = 0, \qquad w = 0, \qquad w_t = 0 \qquad (t = 0), \tag{4}$$

with the pressure (3) being hydrostatic in the channel and zero on the ice-water interface. The total velocity potential, φ_{tot}, satisfies the following boundary conditions on the walls and the bottom of the channel,

$$\varphi_{tot,y} = 0 \quad (y = \pm L), \qquad \varphi_{tot,z} = 0 \quad (z = -H), \tag{5}$$

the kinematic condition on the ice-water interface,

$$\frac{\partial w}{\partial x}\frac{\partial\varphi_{tot}}{\partial x} + \frac{\partial w}{\partial y}\frac{\partial\varphi_{tot}}{\partial y} + \frac{\partial w}{\partial t} = \frac{\partial\varphi_{tot}}{\partial z} \qquad (-\infty < x < \infty,\ -L < y < L,\ z = w(x, y, t)), \tag{6}$$

and the Laplace equation,

$$\nabla^2 \varphi_{tot} = 0, \tag{7}$$

in the flow region except a small vicinity of the dipole, where

$$\varphi_{tot} \sim -I \frac{x - x_0(t)}{r^3}, \qquad r = \sqrt{(x-x_0)^2 + (y-y_0)^2 + (z-z_0)^2} \tag{8}$$

as $r \to 0$ and $t > 0$. Here (x_0, y_0, z_0) are the coordinates of the moving dipole, r is the distance from the dipole and I is the dipole strength. Both the potential $\varphi_{tot}(x, y, z, t)$ and the deflection $w(x, y, t)$ decay with the distance from the dipole at any finite time t,

$$\varphi_{tot} \to 0, \qquad w \to 0 \qquad (|x - x_0(t)| \to \infty), \tag{9}$$

in the model of viscoelastic plate (1).

In the present study, the dipole moves along the channel at a constant speed U and does not move in both z and y directions,

$$z_{0,t} = 0, \qquad y_{0,t} = 0, \qquad x_0 = Ut. \tag{10}$$

The strength of the dipole, I, is a positive constant. In the coordinate system X, y, z, moving together with the dipole, $X = x - Ut$, the dipole is stationary but the fluid moves in the negative x direction with the speed U. The flow close to the dipole is described by the local potential $-IX/r^3 - UX$, where $X = r\cos\theta$ with a polar angle θ. Differentiating the local potential in r and equating the result to zero, we find that the local potential describes the flow around a sphere of radius $R = (2I/U)^{1/3}$. In other words, a rigid sphere of radius R moving in an unbounded fluid at speed U generates a flow which is equivalent to the flow caused by the dipole placed at the centre of a sphere and with strength $UR^3/2$, [19]. The radius R will be used below as a characteristic of the dipole strength. When R is much smaller than the dimensions of the channel cross section, the dipole represents a small sphere moving under the ice cover. If R is comparable with the channel dimensions L and H, the dipole still represents a rigid body moving in the channel when the ice deflection is negligible. However, the shape of the rigid body could be rather complicated. To find the shape of the corresponding body and the pressure on the walls of the channel due to the dipole, we need to determine the velocity potential of the dipole, $\varphi^D(X, y, z)$, moving in the channel with rigid walls at a constant speed U. Note that this potential does not depend on time in the moving coordinate system, once y_0, z_0 and I are constant. The potential $\varphi^D(X, y, z)$ satisfies the Laplace equation, $\varphi^D_{XX} + \varphi^D_{yy} + \varphi^D_{zz} = 0$, in the channel, $(|X| < \infty, |y| < L, -H < z < 0)$, decays at infinity, $\varphi^D \to 0$ as $|X| \to \infty$, and behaves as

$$\varphi^D \sim -\frac{UR^3}{2} \frac{X}{r^3}, \tag{11}$$

where $r = \sqrt{X^2 + (y-y_0)^2 + (z-z_0)^2}$ tends to zero. Its normal derivative is equal to zero on the boundaries of the channel, $y = \pm L$, $z = 0$, and $z = -H$. The potential $\varphi^D(X, y, z)$ is obtained by using the method of images. First, the images of the dipole (11) with respect to the vertical walls of the channel are used to satisfy the boundary conditions at $y = \pm L$. The resulting potential, φ^{D1}, is given by the infinite series,

$$\varphi^{D1}(X, y, y_0, z, z_0) = -\frac{UR^3}{2} X \left\{ \frac{1}{\widetilde{r}^3(y_0, z_0)} + \sum_{n=1}^{\infty} \left[\frac{1}{\widetilde{r}^3(y_0 + 4nL, z_0)} + \right.\right.$$

$$\frac{1}{\widetilde{r}^3((4n-2)L-y_0,z_0)}+\frac{1}{\widetilde{r}^3(y_0-4nL,z_0)}+\frac{1}{\widetilde{r}^3(-(4n-2)L-y_0,z_0)}\Bigg]\Bigg\}, \tag{12}$$

where $\widetilde{r}(y_0,z_0)=\sqrt{X^2+(y-y_0)^2+(z-z_0)^2}$. Note that only the coordinates of the images are shown in $\widetilde{r}(y_0,z_0)$. The potential (12) does not satisfy the boundary conditions at $z=0$ and $z=-H$. The method of images is used for the potential (12) to satisfy these conditions by reflecting φ^{D1} with respect to the planes $z=-H$ and $z=0$. The resulting potential reads

$$\varphi^D(X,y,z)=\varphi^{D1}(X,y,y_0,z,z_0)+\sum_{m=1}^{\infty}\big(\varphi^{D1}(X,y,y_0,z,z_0+2mH)+\varphi^{D1}(X,y,y_0,z,-z_0-2mH)+$$

$$+\varphi^{D1}(X,y,y_0,z,z_0-2mH)+\varphi^{D1}(X,y,y_0,z,-z_0+2(m-1)H)\big). \tag{13}$$

The three-dimensional shape of a body in the channel, which corresponds to the potential (13), is difficult to analyse. It is expected that the shape of the corresponding body is close to a sphere for a dipole of small strength placed in the middle of the channel cross section, and is a deformed sphere for a dipole placed near a wall. By adding dipoles with different strengthes at different points of the channel an underwater object of complex geometry can be modelled.

The potential (13) makes it possible to decompose the total potential of the flow in the channel,

$$\varphi_{tot}(x,y,z,t)=\varphi^D(X,y,z)+\varphi^E(X,y,z,t), \tag{14}$$

where φ^E accounts for elastic deformation of the ice cover in the channel. The ice deflection $w(X+Ut,y,t)$ is denoted by $w^E(X,y,t)$ below. The potential φ^E and the deflection w^E are written in the moving coordinate system. The potential is regular in the flow region, satisfies the Laplace equation,

$$\nabla^2\varphi^E=0 \qquad (-\infty<X<\infty,\ -L<y<L,\ -H<z<w^E(X,y,t)), \tag{15}$$

the boundary conditions on the rigid walls of the channel,

$$\varphi^E_y=0 \qquad (y=\pm L), \qquad \varphi^E_z=0 \qquad (z=-H), \tag{16}$$

the kinematic condition on the ice-water interface,

$$\frac{\partial\varphi^E}{\partial z}+U\frac{\partial w^E}{\partial X}=\frac{\partial w^E}{\partial X}\left(\frac{\partial\varphi^D}{\partial X}+\frac{\partial\varphi^E}{\partial X}\right)+\frac{\partial w^E}{\partial y}\left(\frac{\partial\varphi^D}{\partial y}+\frac{\partial\varphi^E}{\partial y}\right)+\frac{\partial w^E}{\partial t}-\frac{\partial\varphi^D}{\partial z} \qquad (z=w^E(X,y,t)), \tag{17}$$

and decays at infinity as $|X|\to\infty$.

The hydrodynamic pressure in the plate equation (1) is given by the Bernoulli equation (3), where the potential φ_{tot} is provided by (14),

$$p=-\rho_l\left(-U\frac{\partial\varphi^D}{\partial X}-U\frac{\partial\varphi^E}{\partial X}+\frac{\partial\varphi^E}{\partial t}+\frac{1}{2}|\nabla\varphi^D|^2+\nabla\varphi^D\cdot\nabla\varphi^E+\frac{1}{2}|\nabla\varphi^E|^2+gw^E\right) \quad (z=w^E(X,y,t)), \tag{18}$$

where $\nabla\varphi^D=(\partial\varphi^D/\partial X,\partial\varphi^D/\partial y,\partial\varphi^D/\partial z)$. Note that $\partial\varphi^D/\partial z$ is equal to zero on the undisturbed ice-water interface, $z=0$, but not on the actual position of the interface, $z=w^E(X,y,t)$.

We shall determine the solution of the formulated problem (1), (2), (14)–(18) as $t\to\infty$, when both the flow and the ice deflection are independent of time in the moving coordinate system because of the viscoelastic

	Fr	μ	ε
(a)	$\ll 1$	$O(1)$	$O(1)$
(b)	$O(1)$	$\ll 1$	$O(1)$
(c)	$O(1)$	$O(1)$	$\ll 1$

Таблица 1: Conditions of negligible deflection of ice cover.

properties of the ice plate, see equation (1). Then the derivatives of the ice deflection on the left-hand side of the plate equation (1) are transformed as

$$\frac{\partial^2 w}{\partial t^2} \to U^2 \frac{\partial^2 w^E}{\partial X^2},$$

$$\Big(1+\tau\frac{\partial}{\partial t}\Big)\Big(\frac{\partial^4 w}{\partial x^4}+2\frac{\partial^4 w}{\partial x^2\partial y^2}+\frac{\partial^4 w}{\partial y^4}\Big) \to \Big(1-\tau U\frac{\partial}{\partial X}\Big)\Big(\frac{\partial^4 w^E}{\partial X^4}+2\frac{\partial^4 w^E}{\partial X^2\partial y^2}+\frac{\partial^4 w^E}{\partial y^4}\Big).$$

We also should drop the terms $\partial\psi^E/\partial t$ in (18) and $\partial w^E/\partial t$ in (17) in the large-time limit. Note that both the elastic potential and the deflection decay as $|X| \to \infty$ in the model of viscoelastic ice.

We are concerned with small ice deflections, where the linear equation (1) of the ice plate dynamics is justified and a deflection scale, w_{sc}, is much smaller than the characteristic length of the channel L. It is convenient to introduce the characteristic length of the ice cover [1, 3], $L_c = (D/\rho_l g)^{1/4}$, the Froude number $\mathrm{Fr} = U/\sqrt{gL}$, and the non-dimensional parameter, $\varepsilon = R/L$, which describes the strength of the dipole. Then the scale of the potential of the dipole is $\varphi^D_{sc} = UR^3/L^2 = UL\varepsilon^3$, see equations (13) and (14). In the Bernoulli equation (18),

$$\frac{\frac{1}{2}|\nabla\varphi^D|^2}{U\partial\varphi^D/\partial X} \sim \frac{(\varphi^D_{sc}/L)^2}{U\varphi^D_{sc}/L} = \frac{\varphi^D_{sc}}{LU} = \varepsilon^3. \tag{19}$$

Therefore, the quadratic term in (18) with the dipole potential should be retained only if ε is not small. Then the scale of the hydrodynamic pressure is $p_{sc} = \rho_l U^2\varepsilon^3$. Below the non-dimensional variables are denoted by tilde, where $X = L\widetilde{x}$, $y = L\widetilde{y}$, and $z = L\widetilde{z}$. The plate equation (1) in the non-dimensional variables and the moving coordinate system provides

$$\frac{U^2\rho_i h_i w_{sc}}{L^2}\frac{\partial^2\widetilde{w}}{\partial\widetilde{x}^2} + \frac{\rho_l g L_c^4 w_{sc}}{L^4}\left(1-\frac{\tau U}{L}\frac{\partial}{\partial\widetilde{x}}\right)\widetilde{\nabla}^4\widetilde{w} = p_{sc}\widetilde{p}(\widetilde{x},\widetilde{y},\widetilde{w}) - \rho_l g w_{sc}\widetilde{w}, \tag{20}$$

where $\widetilde{p}$ is the non-dimensional dynamic pressure component. We introduce two non-dimensional parameters: non-dimensional retardation time, $\delta = \tau U/L$, and the non-dimensional rigidity of the ice cover, $\mu = L/L_c$. Here L_c is independent of the channel dimensions and depends on the ice thickness h_i. If $\mu = O(1)$, then the support of the ice cover through the ice edge conditions on the walls of the channel plays an important role. However, if the channel is wide, $\mu \gg 1$, than the ice cover is mainly supported by the buoyancy force. Therefore, the bending stresses balance the pressure $\widetilde{p}p_{sc}$ for narrow channels, and then $\rho_l g w_{sc}/\mu^4 = p_{sc}$ for $\mu = O(1)$ including $\mu \ll 1$. Correspondingly the buoyancy force plays the main role and $\rho_l g w_{sc} = p_{sc}$ for $\mu \gg 1$. Both cases can be combined in a single formula for the scale of ice deflection,

$$w_{sc} = L\,\mathrm{Fr}^2\varepsilon^3\min(\mu^4, 1). \tag{21}$$

The condition of small deflection, $w_{sc}/L \ll 1$, is satisfied when at least one of the parameters $\mathrm{Fr}, \mu, \varepsilon$ is small, see Table 1. Each case is considered separately below.

(a) Slow motion of the dipole

In this case, $w_{sc}/L = O(\mathrm{Fr}^2)$, $\mathrm{Fr} = o(1)$ and $\varepsilon = O(1)$. The kinematic condition (17) provides the scale of the elastic potential, φ^E_{sc}, by comparing the orders of the terms on the left-hand side of (17) and using (21),

$$\varphi^E_{sc} = U w_{sc}. \tag{22}$$

The relative order of the potentials φ^D and φ^E is

$$\frac{\varphi^E_{sc}}{\varphi^D_{sc}} = \frac{U w_{sc}}{U L \varepsilon^3} = \mathrm{Fr}^2 \mu^4.$$

This implies that φ^E can be neglected compared with φ^D in the Bernoulli equation (18), making the dynamic pressure to be independent of the ice deflection in leading order. Therefore, the problem is decoupled for small Froude numbers. The inertia term in (20) can be neglected in leading order compared with the hydrodynamic pressure term,

$$\frac{U^2 \rho_i h_i w_{sc}}{L^2 p_{sc}} = \alpha \mathrm{Fr}^2 \mu^4, \quad \alpha = \frac{\rho_i h_i}{\rho_l L},$$

where $\alpha = O(1)$ and $\mathrm{Fr} \ll 1$. Then the equation (20) for the non-dimensional deflection $\widetilde{w}(\widetilde{x}, \widetilde{y})$ reads in leading order

$$\left(1 - \delta \frac{\partial}{\partial \widetilde{x}}\right) \widetilde{\nabla}^4 \widetilde{w} + \mu^4 \widetilde{w} = \frac{\partial \widetilde{\varphi}^D}{\partial \widetilde{x}} - \frac{1}{2} \varepsilon^3 |\widetilde{\nabla} \widetilde{\varphi}^D|^2. \tag{23}$$

This static equation of the ice deflection in the moving coordinate system should be solved subject to the boundary conditions (2) on the walls of the channel, $\widetilde{y} = \pm 1$, and the condition (9) as $\widetilde{x} \to \pm\infty$. The equation (23) can be additionally simplified for narrow channels, $\mu \ll 1$, and/or for weak dipole, $\varepsilon \ll 1$. Once the ice deflection $\widetilde{w}(\widetilde{x}, \widetilde{y})$ has been determined, one can find the elastic potential $\widetilde{\varphi}^E(\widetilde{x}, \widetilde{y}, \widetilde{z})$ in the leading order as $\mathrm{Fr} \to 0$ by solving the boundary problem (14) – (17) in the linearized flow region, $\widetilde{y} < 1$, $-h < \widetilde{z} < 0$, $|\widetilde{x}| < \infty$, where $h = H/L$. The most complicated part of this problem is the kinematic condition (17) in leading order as $\mathrm{Fr} \to 0$. The derivative $\partial \varphi^D / \partial z$ on the boundary, $\widetilde{z} = \widetilde{w}(\widetilde{x}, \widetilde{y})$, in this condition is approximated as

$$\frac{\partial \varphi^D}{\partial z}(X, y, w) \approx \frac{\partial^2 \varphi^D}{\partial z^2}(X, y, 0) w = -\nabla_2^2 \varphi^D(X, y, 0) w =$$

$$-\frac{U \varepsilon^3}{L} w_{sc} \widetilde{\nabla}_2^2 \widetilde{\varphi}^D(\widetilde{x}, \widetilde{y}, 0) \widetilde{w}.$$

As a result the condition (17) reads in leading order,

$$\frac{\partial \varphi^E}{\partial \widetilde{z}} = \frac{\partial \widetilde{w}}{\partial \widetilde{x}} + \varepsilon^3 \left[\frac{\partial \widetilde{w}}{\partial \widetilde{x}} \frac{\partial \widetilde{\varphi}^D}{\partial \widetilde{x}} + \frac{\partial \widetilde{w}}{\partial \widetilde{y}} \frac{\partial \widetilde{\varphi}^D}{\partial \widetilde{y}} + \widetilde{\nabla}_2^2 \widetilde{\varphi}^D \widetilde{w} \right], \tag{24}$$

where $\widetilde{\varphi}^D$ is given by (13) and $\widetilde{w}(\widetilde{x}, \widetilde{y})$ is the solution of the problem (23), (2). The Neumann boundary problem (14) – (16), (24) has a solution only if the integral of the right-hand side in (24) over the ice cover is zero. It is straightforward to show that the total flux through the ice-water interface indeed is equal to zero by using the edge conditions (2) and the condition (9) that the ice deflection $\widetilde{w}$ and the flow potential $\widetilde{\varphi}^D$ decay at infinity, $\widetilde{x} \to \pm\infty$.

Equations (23) and (24) show that ε is the parameter of linearization. The buoyancy term in (23) can be neglected in leading order for narrow channels with $\mu \ll 1$. For zero speed of the dipole, the dipole strength I cannot be related to the radius of a sphere in unbounded flow. In this case, $\varphi^D_{sc} = I/L^2$ and a characteristic speed $U_{sc} = I/L^3$ can be introduced. Then the results of this section are still valid but with the dipole speed U

replaced by U_{sc} and $\varepsilon = 1$. In addition, we should set $\delta = 0$ and $\partial\widetilde{\varphi}^D/\partial\widetilde{x} = 0$ in (23), and $\partial\widetilde{w}/\partial\widetilde{x} = 0$ in (24). The approximation of slow dipole is valid for $I/(L^3\sqrt{gL}) \ll 1$.

(b) Narrow channel

In this case, $w_{sc}/L = O(\mu^4)$ as $\mu \to 0$. The relation (22) is valid in this case as well. The elastic potential can be neglected compared with the potential of the dipole when $\mathrm{Fr}^2\mu^4 \ll 1$. The ice deflection is described by (23) in leading order, where the buoyancy term $\mu^4\widetilde{w}$ should be dropped. The kinematic condition (24) keeps its form in leading order.

We conclude that for narrow channels with $L/L_c \ll 1$ the ice deflection is described by the static equation (23) without the buoyancy term. Therefore, the problem is decoupled. The relative correction to the hydrodynamic pressure, and respectively to the ice cover deflection, is of order $\varphi^E_{sc}/\varphi^D_{sc} = O(\mathrm{Fr}^2\mu^4)$ in both (a) and (b) cases.

(c) Weak dipole

The case of a small rigid body, $R/L \ll 1$, moving along the channel provides $w_{sc}/L = O(\varepsilon^3)$. For $\mathrm{Fr} = O(1)$ and $\mu = O(1)$ the elastic potential φ^E and the potential of the dipole, φ^D, are of the same order. Therefore, the problem is coupled in this case, see equation (18). However, the quadratic terms in (18) can be neglected in leading order, see (19). The relation (22) is valid in this case as well. The terms on the right-hand side of (17) can be neglected. They are of order $O(\varepsilon^3)$ as $\varepsilon \to 0$. For a weak dipole, the problem is coupled but linear. The inertia term in the plate equation (20), in general, cannot be neglected. The plate equation in this case reads

$$\alpha\mathrm{Fr}^2\frac{\partial^2\widetilde{w}}{\partial\widetilde{x}^2} + \frac{1}{\mu^4}\left(1 - \delta\frac{\partial}{\partial\widetilde{x}}\right)\widetilde{\nabla}_2^4\widetilde{w} + \widetilde{w} - \mathrm{Fr}^2\frac{\partial\widetilde{\varphi}^E}{\partial\widetilde{x}} = \frac{\partial\widetilde{\varphi}^D}{\partial\widetilde{x}}(\widetilde{x},\widetilde{y},0) \quad (\widetilde{z}=0, |\widetilde{y}|<1, |\widetilde{x}|<\infty). \tag{25}$$

This equation should be solved subject to the edge conditions (2) and the condition (9) far from the dipole, $\widetilde{x} \to \pm\infty$. The potential of the dipole, $\widetilde{\varphi}^D$, in (25) is given by (13) and (14). The elastic potential $\widetilde{\varphi}^E$ is the solution of the Neumann problem (16) – (18) with the condition,

$$\frac{\partial\widetilde{\varphi}^E}{\partial\widetilde{z}} = -\frac{\partial\widetilde{w}}{\partial\widetilde{x}} \quad (\widetilde{z}=0, |\widetilde{y}|<1, |\widetilde{x}|<\infty), \tag{26}$$

on the ice-water interface. The approximation of a weak dipole is the most complex one because the ice deflection and the flow under the ice are coupled in this case.

3. The ice deflection by a weak dipole

The coupled linear problem (1), (15) – (17), (25), (26) is solved by using the Fourier transform in the $\widetilde{x}$-coordinate along the channel and the normal mode method with beam functions in the $\widetilde{y}$-coordinate across the channel. This problem is similar to the problem of an external load moving along the channel at a constant speed. The external load is represented by the derivative $(\partial\widetilde{\varphi}^D/\partial\widetilde{x})(\widetilde{x},\widetilde{y},0)$ on the right hand-side of the ice plate equation (25), see equation (6) in [3]. Similarly to the analysis of [3], after the Fourier transform along the channel, the term $-\mathrm{Fr}^2\partial\widetilde{\varphi}^E/\partial\widetilde{x}$ in (25) can be represented by an added-mass matrix for clamped beam modes, and the plate equation (25) can be reduced to a system of algebraic equations for the coefficients of the series of the ice deflection $\widetilde{w}(\widetilde{x},\widetilde{y})$ with respect to the beam modes.

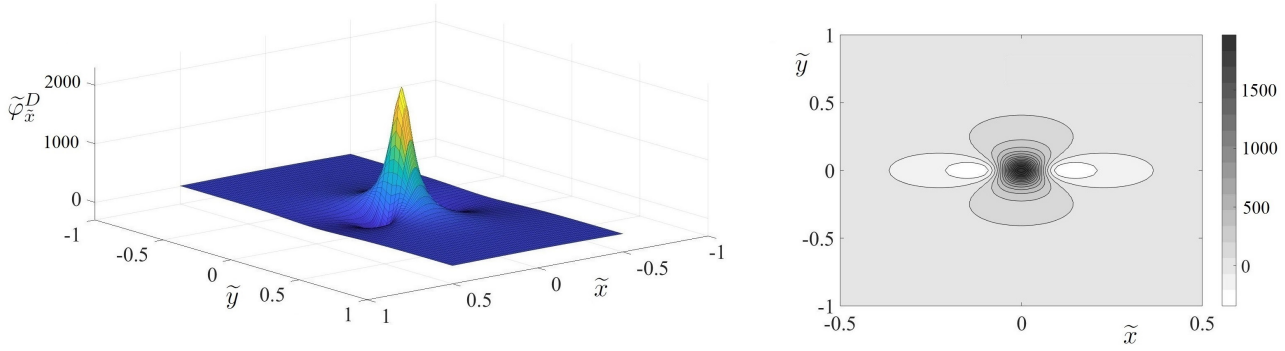

Рис. 2: The non-dimensional forcing term $\widetilde{\varphi}^D_{\tilde{x}}(\tilde{x},\tilde{y},0,0,-h/2)$ in (27) for $\widetilde{y}_0=0$ and $\widetilde{z}_0=-h/2$, where $h=0.2$.

The non-dimensional equations describing the ice plate deflection in the coordinate system moving together with a weak dipole along the channel read

$$\alpha \mathrm{Fr}^2 \widetilde{w}_{\tilde{x}\tilde{x}} + \frac{1}{\mu^4}\left(1-\delta\frac{\partial}{\partial\widetilde{x}}\right)\nabla_2^4\widetilde{w} + \widetilde{w} - \mathrm{Fr}^2\widetilde{\varphi}^E_{\tilde{x}} =$$

$$= \widetilde{\varphi}^D_{\tilde{x}}(\widetilde{x},\widetilde{y},\widetilde{y}_0,0,\widetilde{z}_0) \qquad (|\widetilde{x}|<\infty,\ \ |\widetilde{y}|<1), \tag{27}$$

$$\widetilde{w}=0, \quad \widetilde{w}_{\tilde{y}}=0 \qquad (\widetilde{y}=\pm 1), \tag{28}$$

$$\nabla^2\widetilde{\varphi}^E = 0 \qquad (-\infty<\widetilde{x}<\infty,\ \ -1<\widetilde{y}<1,\ \ -h<\widetilde{z}<0), \tag{29}$$

$$\widetilde{\varphi}^E_{\tilde{z}} = -\widetilde{w}_{\tilde{x}} \quad (\widetilde{z}=0), \qquad \widetilde{\varphi}^E_{\tilde{z}}=0 \quad (\widetilde{z}=-h), \qquad \widetilde{\varphi}^E_{\tilde{y}}=0 \quad (\widetilde{y}=\pm 1), \tag{30}$$

$$\widetilde{\varphi}^E \to 0, \quad \widetilde{w}\to 0 \qquad (|\widetilde{x}|\to\infty). \tag{31}$$

The potential $\widetilde{\varphi}^D$ in the right-hand side of (27) is given by (13) written in the dimensionless variables. Note that $\widetilde{\varphi}^D_{\tilde{x}}(\widetilde{x},\widetilde{y},\widetilde{y}_0,0,\widetilde{z}_0)$ is even in $\widetilde{x}$. It is also even in $\widetilde{y}$ for $\widetilde{y}_0=0$. The forcing term, $\widetilde{\varphi}^D_{\tilde{x}}(\widetilde{x},\widetilde{y},0,0,-h/2)$, is depicted in Figure 2 for a dipole moving at the middle of the channel cross section, where $h=0.2$.

The solution of the stationary problem (27) – (31) depends on four non-dimensional parameters, α, Fr, μ, δ, and the non-dimensional coordinates of the dipole, $\widetilde{y}_0$, $\widetilde{z}_0$. We shall determine the steady state ice deflection, $\widetilde{w}(\widetilde{x},\widetilde{y})$, and the distribution of strains in the ice plate, $\widetilde{\varepsilon}(\widetilde{x},\widetilde{y})$, for some typical values of the parameters of the problem.

We are concerned, in particular, with the effect of the dipole position in the channel on the ice deflections and strain distribution in the ice cover. The ice deflection and strains are scaled with w_{sc} given in equation (21) and $\epsilon_{sc}=h_i w_{sc}/(2L^2)$ correspondingly. These scales depend on the dipole strength through the parameter ε.

In the linear theory of hydroelasticity, the strains vary linearly through the ice thickness and are zero at the middle of the plate thickness. This model is known as the Kirchhoff plate model. At any location in the plate, the maximum strain is achieved on either upper or lower surface of the plate. We are concerned with positive strains which correspond to elongations of the ice surface and tensile stresses in the ice. The strain tensor is given by

$$\widetilde{E}(\widetilde{x},\widetilde{y}) = -\zeta\begin{pmatrix} \widetilde{w}_{\tilde{x}\tilde{x}} & \widetilde{w}_{\tilde{x}\tilde{y}} \\ \widetilde{w}_{\tilde{x}\tilde{y}} & \widetilde{w}_{\tilde{y}\tilde{y}} \end{pmatrix}, \tag{32}$$

where ζ is the non-dimensional coordinate across the ice thickness, $-1\le\zeta\le 1$, and the matrix with the second-order partial derivatives describes the local curvature of the plate surface, $\widetilde{z}=\widetilde{w}(\widetilde{x},\widetilde{y})$, see [5]. To find

the maximum strain in the ice sheet, we need to determine the eigenvalues of the strain tensor at each location over the ice sheet and take the maximum of them in magnitude. The linear theory of hydroelasticity can be used when the strains are below the yield strain ϵ_{cr} of the ice. The yield strain of a material is defined as the strain at which the material begins to deform plastically [24]. Strains greater than the yield strain may lead to ice fracture. The fracture strain in the experiments with ice was reported as $3 \cdot 10^{-5}$, and the theory predicts ice fracture when the strain reaches $4.3 \cdot 10^{-5}$, see [25]. In the present study, we use the estimate $\epsilon_{cr} = 8 \cdot 10^{-5}$, see [26] and discussion of this value there.

The problem (27) – (31) is solved using the Fourier transform in the $\widetilde{x}$-direction,

$$\widetilde{w}^F(\xi,\widetilde{y}) = \frac{1}{\sqrt{2\pi}} \int\limits_{-\infty}^{\infty} \widetilde{w}(\widetilde{x},\widetilde{y}) e^{-i\xi\widetilde{x}} d\widetilde{x}, \qquad \widetilde{w}(\widetilde{x},\widetilde{y}) = \frac{1}{\sqrt{2\pi}} \int\limits_{-\infty}^{\infty} \widetilde{w}^F(\xi,\widetilde{y}) e^{i\xi\widetilde{x}} d\xi.$$

The Fourier transform applied to the plate equation (27) and the boundary conditions (28) provides

$$-\alpha \mathrm{Fr}^2 \xi^2 \widetilde{w}^F + \frac{1}{\mu^4}\left(1 - i\delta\xi\right)\left(\widetilde{w}^F_{\widetilde{y}\widetilde{y}\widetilde{y}\widetilde{y}} - 2\xi^2 \widetilde{w}^F_{\widetilde{y}\widetilde{y}} + \xi^4 \widetilde{w}^F\right) + \widetilde{w}^F - i\xi \mathrm{Fr}^2 (\widetilde{\varphi}^E)^F =$$

$$= i\xi (\widetilde{\varphi}^D)^F(\xi,\widetilde{y},\widetilde{y}_0,0,\widetilde{z}_0) \qquad (-1 < \widetilde{y} < 1), \tag{33}$$

$$\widetilde{w}^F = 0, \quad \widetilde{w}^F_{\widetilde{y}} = 0 \qquad (\widetilde{y} = \pm 1). \tag{34}$$

The function $\widetilde{w}^F(\xi,\widetilde{y})$ is sought in the form of the infinite series,

$$w^F(\xi,\widetilde{y}) = \sum_{j=1}^{\infty} a_j(\xi)\psi_j(\widetilde{y}), \tag{35}$$

where the principal coordinates $a_j(\xi)$ are to be determined, and $\psi_j(\widetilde{y})$ are the non-trivial solutions of the spectral problem,

$$\psi_j^{IV} = \lambda_j^4 \psi_j \quad (-1 < \widetilde{y} < 1), \qquad \psi_j = \psi_j' = 0 \quad (\widetilde{y} = \pm 1), \tag{36}$$

$$\int\limits_{-1}^{1} \psi_i(\widetilde{y})\psi_j(\widetilde{y}) d\widetilde{y} = \delta_{ij},$$

where $\delta_{ij} = 0$ for $i \neq j$ and $\delta_{jj} = 1$, and λ_j are the eigenvalues of the problem (36), $j \geq 1$. The functions $\psi_j(\widetilde{y})$ are known as clamped beam modes [5] . We distinguish even modes, $\psi_j^c(\widetilde{y})$, and odd modes, $\psi_j^s(\widetilde{y})$, where $\psi_j^c(-\widetilde{y}) = \psi_j^c(\widetilde{y})$ and $\psi_j^s(-\widetilde{y}) = -\psi_j^s(\widetilde{y})$ for $-1 < \widetilde{y} < 1$ and $j \geq 1$.

We consider a dipole placed either at the centre line of the channel, where $\widetilde{y}_0 = 0$, or closer to a wall. For a dipole moving along the centre line of the channel the solution of (33) and (34) is even in $\widetilde{y}$. Therefore, only the even modes should be included in the series (35) in this case. The even and odd modes do not interact with each other and the series (35) can be detailed, in general, as

$$\widetilde{w}^F(\xi,\widetilde{y}) = \sum_{j=1}^{\infty} a_j^c(\xi)\psi_j^c(\widetilde{y}) + \sum_{j=1}^{\infty} a_j^s(\xi)\psi_j^s(\widetilde{y}), \tag{37}$$

where a_j^c and a_j^s are principal coordinates of the even and odd modes, respectively. Substituting (37) in the equation (33), multiplying both sizes of the equation by $\psi_j^c(\widetilde{y})$, and integrating the result in $\widetilde{y}$ from -1 to 1, using the orthogonality condition from (36), we arrive at an infinite system of linear equations for $a_j^c(\xi)$. Note that the term $-i\xi(\widetilde{\varphi}^E)^F$ in (33) with the elastic potential leads to the matrix of added masses for the clamped beam

modes, see [5]. The obtained algebraic system is solved by the truncation method. A similar procedure with odd modes $\psi_j^s(\widetilde{y})$ leads to a system of linear equations for the coefficients $a_j^s(\xi)$. Finally, the ice deflection $\widetilde{w}(\widetilde{x},\widetilde{y})$ is determined using the inverse Fourier transform. Finite numbers of terms, N_{mod}^c and N_{mod}^s, are retained in the series (37) in numerical calculations. The inverse Fourier transforms of the coefficients in (37) are evaluated numerically using linear interpolation of the coefficients. Note that the clamped beam modes are independent of the parameter ξ of the Fourier transform. For more details of the numerical solution see [3].

4. Numerical results

The hydroelastic behaviour of the ice cover in a channel, which is caused by a dipole moving under the ice, is investigated numerically for a freshwater ice with density $\rho_i = 917$ kg/m^3, Young's modulus $E = 4.2\cdot 10^9$ N/m^2, Poisson's ratio $\nu = 0.3$ and the retardation time $\tau = 0.1$ s, the thickness of the ice plate $h_i = 10$ cm, the half width of the channel $L = 10$ m and the water depth $H = 2$ m. These conditions were used in [5]. The coordinates of the dipole are (X, y_0, z_0) in the original dimensional variables, $X = Ut$. The speed U and the position of the dipole with respect to the walls of the channel, y_0 and z_0, vary in the present calculations. In contrast to the problem of a dipole moving under ice sheets of infinite extent, there are infinitely many critical speeds of hydroelastic waves in the frozen channel. Correspondingly, there are many values of the speed of the moving dipole at which the strains in the ice cover peak. The strains are finite even at the critical speeds because of the viscoelastic properties of the ice cover. The ranges of the speeds U in the numerical analysis are related to the critical speeds of the hydroelastic waves propagating in the frozen channel. These speeds were computed in [5]. The characteristic length L_c of the ice cover is equal to 2.48 m in the case under consideration. For such a characteristic length the presence of the side walls of the channel is important for both strains and deflections as was shown in [3], see Figures 9 and 10 there. The lowest critical speed for this channel is 5.38 m/s for $\tau = 0$ s and approximately 5.5 m/s for $\tau = 0.1$ s, see [3]. In this section, we investigate elastic behaviour of the ice cover for speeds of the dipole near the first critical speed.

Calculations of the deflection, $\widetilde{w}(\widetilde{x},\widetilde{y})$, and the strains by (32) require numerical evaluations of the inverse Fourier transforms of the functions $a_j^c(\xi)$ and $a_j^s(\xi)$ in series (37). In total, $3(N_{\rm mod}^c + N_{\rm mod}^s)$ integrals should be evaluated for different values of the $\widetilde{x}$-coordinate along the channel. The number of the modes retained in each series of (37) varies from 5 to 15 to confirm the convergence of both series (37) and the corresponding series for the strains. For the conditions of the calculations, accurate evaluation of the inverse Fourier transforms was achieved by limiting the integration intervals to (0, 200) with variable steps of integration from 0.1 to 1. The dipole potential, $\varphi^D(x, y, y_0, 0, z_0)$, on the ice-water interface is determined by the double series (12) and (13). The series quickly converge. The number of terms in each series, N_{dip}, varies from 10 to 1000 to confirm accuracy of the numerical results. The right-hand side of equation (33) is shown in Fig. 3 for two different distances of the dipole from the ice cover. It is seen that the forcing load is localised near the dipole in the $\widetilde{y}$-direction. However, the load slowly decays with increase of the parameter ξ of the Fourier transform.

As a reference case, we consider a dipole of strength I, see equation (8), corresponding to a sphere of radius $R = 30$ cm moving in unbounded fluid. The diameter of such a sphere is smaller than the channel depth. The dipole strength, $I = UR^3/2$, depends on the body speed U, see [19]. Then $\varepsilon = R/L = 0.03$, and

$\mu = L/L_c = 4.02$ is greater than one in (21). The numerical results below are presented in the dimensional variables for the constant radius $R = 30$ cm and different speeds of the dipole, U. Note that the problem in the dimensionless variables, see equation (25), depends on the speed of the dipole U, but not on the radius R. Correspondingly, the strains and deflections presented below can be multiplied by the factor $(\widetilde{R}/0.3m)^3$ to obtain the results for an arbitrary radius $\widetilde{R}$ and strength $I = U\widetilde{R}^3/2$ of the dipole. As it mentioned in Introduction, for a dipole moving relatively close to a wall, the shape of the corresponding rigid body is not spherical and can be determined. In any case this fictitious body is inside the channel and does not touch the channel walls.

The ice deflections and strains are shown in Figs. 4 - 6 for the dipole moving along the centre of the channel, $y_0 = 0$, at different levels below the ice cover, $|z_0| = 7H/8$, $3H/4$, $H/2$, $H/4$, $H/8$ m, and at speeds 3 and 7 m/s. For the subcritical speed of the dipole, $U = 3$ m/s, the ice deflections and strains are shown in Fig. 4 and Fig. 5, respectively. In the subcritical case, both the deflections and strains are even functions of X and y. The strains at the central line, see Fig. $5b$, are always higher than the strains along the walls of the channel, see Fig. $5c$. For the dipole moving at the depth $H/4 = 50$ cm beneath the ice at this subcritical speed, the maximum strain $2 \cdot 10^{-5}$, see Fig. $5b$, is achieved above the dipole. By using the scaling factor $(\widetilde{R}/0.3m)^3$, we conclude that the maximum strain approaches the yield strain $\epsilon_{cr} = 8 \cdot 10^{-5}$ for the dipole corresponding to a sphere of radius 47 cm in unbounded fluid, moving at speed 3 m/s.

The strains for a supercritical speed of the dipole, $U = 7\text{m/s}$, are shown in Fig. 6 for different distances of the dipole below the ice cover. An important difference between the subcritical case, see Figs. 4, 5, and the supercritical case, see Fig. 6, is the wave in the ice cover generated by the dipole in front of it. This is in agreement with the theory of large-time response of the ice cover to a load moving along a frozen channel, [28]. The strains approach the yield strain, $\epsilon_{cr} = 8 \cdot 10^{-5}$, in front of the dipole, if the strength I of the dipole is increased about 4 times. This implies that a dipole, the strength of which is equivalent to a sphere of radius 35 cm in the unbounded fluid, moving at speed 7 m/s at depth 0.5 m may break the ice cover of thickness 10 cm about 3 m in front of it, see Fig. 6 *b*. The Fig. 6 shows also that the strains at the wall at $X = 0$, are greater than the strain above the moving dipole if the depth of the dipole submergence is greater than 1 m.

The effect of the dipole position in the channel on the ice deflection and strains is depicted in Figs. 7 and 8, respectively. In these figures, the dipole moves at depth 1 m. The effect of the dipole position with respect to the centre line of the channel is different for different speeds of the dipole. Fig. 7*a* shows that for the subcritical speed $U = 3$ m/s the maximum deflection of the ice above the dipole, $X = 0$, increases with the distance of the dipole from the nearest wall. However, for the supercritical speed $U = 7$ m/s, see Fig. 7*b*, the dipole moving close to a wall may generate larger ice deflection than the dipole moving at the centre of the channel. Moreover, the deflection is maximum near another wall.

The strains, $\epsilon(0, y)$, above the dipole moving at the subcritical speed $U = 3$m/s are shown in Fig. 8*a*. It is seen that the strains monotonically decrease with the distance from the dipole in the main part of the ice cover and increase near the wall. A similar effect is observed for the supercritical speed $U = 7$m/s but now the maximum strain along the channel is shown as a function of y in Fig. 8*b*. We may conclude that the ice cover is more likely to break at the wall but not above the dipole, if the dipole moves closer to one of the channel wall. For larger speed, $U = 12$ m/s, the maximum of the strain is always achieved at the wall for $y_0 \geq 2$ m. Therefore, for supercritical speeds the dipole generates complex deflection of the ship-wave type both behind and in front of it, which is strongly affected by the asymmetry of the dipole trajectory in the channel.

The deflections $w(X, y)$ and strains $\epsilon(X, y)$ of the ice sheet for $y_0 = 8$ m, $|z_0| = 1$ m and $U = 12$ m/s are shown in Fig. 9 as three-dimensional surfaces and as contour plots. Here $h_i = 0.06$ m and $\tau = 0.07$ s. Note the waves both in front and behind the dipole and the Kelvin ship-wave pattern of the waves. One can see reflections of the waves from the distant wall and increase of the strains at the nearest wall of the channel.

Numerical results by the present model are compared with the results from [7], where the motion of a dipole under the ice sheet of infinite extent in the water of infinite depth was studied. In [7], the dipole modelled a sphere of radius $R = 0.5$ m moving at constant speed 6 m/s at distance 5 m beneath the ice cover. The ice thickness h_i was varied from 0.2 to 0.5 m. Other parameters were as follows: water density $\rho_l = 1025$ kg/m^2, ice density $\rho_i = 0.9\rho_l$, Young modulus of ice $E = 3 \times 10^9$ N/m^2, Poisson's ratio $\nu = 0.3$. The pre-existing tensile stress in the ice was accounted in the model of [7] being equal to 10^5 N/m^2. For these conditions the critical velocity of the dipole motion was equal to 8.22 m/s for $h_i = 0.2$ m, and 11.43 m/s for $h_i = 0.5$ m, see [7].

Our calculations were performed for the ice channel of width 120 m and depth 60 m. The parameters of the ice and dipole were the same as in [7], see above. The characteristic length of the ice sheet L_c is estimated as 7.65 m for $h_i = 0.5$ m. In our calculations it was about 8 times smaller then the distance from the dipole to the channel walls. There are no pre-existing stresses in the present model. However, our estimates show that, in the equation of the ice deflection, see equation (1.7) in [7], the term corresponding to the membrane stresses is much smaller that the term describing the bending stresses in the ice cover. This is confirmed by our calculations without account for the membrane stresses. The relatively difference between our deflections and the deflections predicted in [7] is less that 4% for ice thicknesses $h_i = 0.3$, 0.4, and 0.5 m. It should be noticed that the walls of the channel play negligible role in this case, because the dipole moves at subcritical speed and deflection of the ice is localised above the dipole.

5. Conclusion

The deflections and strains of the ice cover in a channel, which are caused by a dipole moving under the ice along the channel, have been investigated. The moving dipole approximately corresponds to a sphere, the radius of which is much smaller than both the depth and the width of the channel. It was shown that the problem of ice deflection is decoupled and linear in leading order. The problem was solved in two steps. First, the ice deflection was neglected and the potential flow generated by the dipole was determined by the method of images for the channel covered with a rigid plate. The solution of this problem provides the hydrodynamic pressure over the rigid upper cover of the channel. Second, this hydrodynamic pressure was taken as a forcing load in the problem of ice deflection caused by the dipole and the flow due to the elastic deflection of the ice cover. The problem was formulated for a visco-elastic ice model in the coordinate system moving together with the dipole, where the ice deflection is stationary for large times. This coupled problem was solved numerically by using the Fourier transform along the channel and the normal modes across the channel. The strains in the ice cover were shown to be strongly dependent on the speed of the dipole and asymmetry of the dipole trajectory. The ice can be broken by the moving dipole either in front of it or on the wall if the dipole moves close to the wall.

The asymptotic analysis revealed two other limiting cases with small ice deflection. In the first case, the channel width is much smaller than the characteristic length of the ice cover, and the ice response is independent of the elastic potential and the buoyancy force in leading order. In the second case, the dipole moves at a small speed with the Froude number being small. In this limiting case, the elastic potential also can be neglected in leading order but the buoyancy force matters.

The characteristic length of the ice cover in calculations of section 4 is four times smaller than the half-length of the channel. However the effect of the side walls of the channel on the strains is significant.

Acknowledgement

The authors thank the Isaac Newton Institute for Mathematical Sciences for support and hospitality during the scientific programme "Mathematics of sea ice phenomena" in August-December 2017, when this study started.

[1] V. Squire, R. Hosking, A. Kerr, P. Langhorne, Moving loads on ice plates, Kluwer Academic Publishers, 1996.

[2] P. Brocklehurst, Hydroelastic waves and their interaction with fixed structures (PhD thesis), University of East Anglia, UK, 2012.

[3] K. Shishmarev, T. Khabakhpasheva, A. Korobkin, The response of ice cover to a load moving along a frozen channel, Applied Ocean Research, 59 (2016) 313-326.

[4] K. Shishmarev, Problem formulation of ice plate viscoelastic oscillations in a channel caused by a moving load, The news of Altai State University, 85 (2015), 189-194 (in Russian).

[5] A. Korobkin, T. Khabakhpasheva, A. Papin, Waves propagating along a channel with ice cover, Eur. J. Mech. B/Fluids 47 (2014), 166-175.

[6] E. Batyaev, T. Khabakhpasheva, Hydroelastic waves in channel with free ice cover, Fluid Dyn. 6 (2015), 84-101.

[7] A.A. Savin, A.S. Savin, Three-dimensional problem of disturbing an ice cover by a dipole moving in fluid, Fluid Dyn. 50 (2015), 613-620.

[8] A.A. Savin A.S. Savin, Ice cover perturbations by a dipole in motion within a liquid, Fluid Dyn. 47 (2012), 139-146.

[9] A.T. Il'ichev, A.S. Savin, Process of establishing a plane-wave system on ice cover over a dipole moving uniformly in an ideal fluid column, Theor. and Math. Phys. 193 (2017), 1801-1810.

[10] A.A. Savin, A.S. Savin, Waves generated on an ice cover by a source pulsating in fluid, Fluid Dyn. 48 (2013), 303-309.

[11] Z.F. Li, Y.Y. Shi G.X. Wu, Large amplitude motions of a submerged circular cylinder in water with an ice cover, Eur. J. Mech. B/Fluids 65 (2017), 141-159.

[12] A.V. Pogorelova, V.M. Kozin, V.L. Zemlyak, Motion of a slender body in a fluid under a floating plate, J. Appl. Mech. Tech. Phys. 53 (1) (2012), 27-37.

[13] A.V. Pogorelova, Unsteady motion of a source in a fluid under a floating plate, J. Appl. Mech. Tech. Phys. 52 (5) (2011), 717Ц726.

[14] I.V. Sturova and L.A. Tkacheva, Oscillations of a submerged cylinder in water with non-homogeneous ice cover, in: Proc. of the Third International Scientific Conference Polar Mechanics. Vladivostok. Russia. (2016), 976-985.

[15] I.V. Sturova, Radiation of waves by a cylinder submerged in water with ice floe or polynya, J. Fluid Mech. 784 (2015), 373-95.

[16] L.A. Tkacheva, Oscillations of a cylindrical body submerged in a fluid with ice cover, J. Appl. Mech. Tech. Phys. 56 (6) (2015), 1084-1095.

[17] Z.F. Li, G.X. Wu, C.Y. Ji, Wave radiation and diffraction by a circular cylinder submerged below an ice sheet with a crack, J. Fluid Mech. 845 (2018), 682-712.

[18] Z.F. Li, G.X. Wu, C.Y. Ji, Interaction of wave with a body submerged below an ice sheet with multiple arbitrarily spaced cracks. Physics of Fluids, 30 (5) (2018), 057107.

[19] N.E. Kochin, I.A.Kibel, N.V.Roze, Theoretical hydromechanics, Interscience. New York, 1964.

[20] K. Shishmarev, T. Khabakhpasheva and A. Korobkin, Hydroelastic waves caused by a load moving along a frozen channel, in: Proc. 7th Intern. Conf. of Hydroelasticity in Marine Technology, Split. Croatia. (2015) 149-160.

[21] T. Miloh, Mathematical Approaches in Hydrodynamics. Philadelphia: Society for Industrial and Applied Mathematics, 1991.

[22] J.N. Newman, Marine Hydrodynamics, Cambridge: The MIT Press, 1977.

[23] S. Timoshenko, S. Woinowsky-Krieger, Theory of Plates and Shells. 2nd ed., McGraw-Hill, New York, U.S.A., 1959.

[24] E. Oberg, F.D. Jones, H.L. Horton, H.H. Ryffel, J.H. Geronimo, Machinery's handbook, 27th edn, Industrial Press Inc, New York, 2004.

[25] D. Goodman, P. Wadhams, V. Squire, The flexural response of a tabular ice island to ocean swell, Ann. Glaciology 1 (1980) 23-27.

[26] P. Brocklehurst, A. Korobkin, E.Părău, Interaction of hydro-elastic waves with a vertical wall, J. Eng. Math. 68 (2010) 215-231.

[27] M. Abramowitz, I.A. Stegun, Handbook of mathematical functions with formulas, graphs, and mathematical tables. Dover Publications, New York (1972).

[28] T. Khabakhpasheva, K. Shishmarev, A. Korobkin, Large-time response of ice cover to a load moving along a frozen channel, Applied Ocean Research, 86 (2019) 154-165.

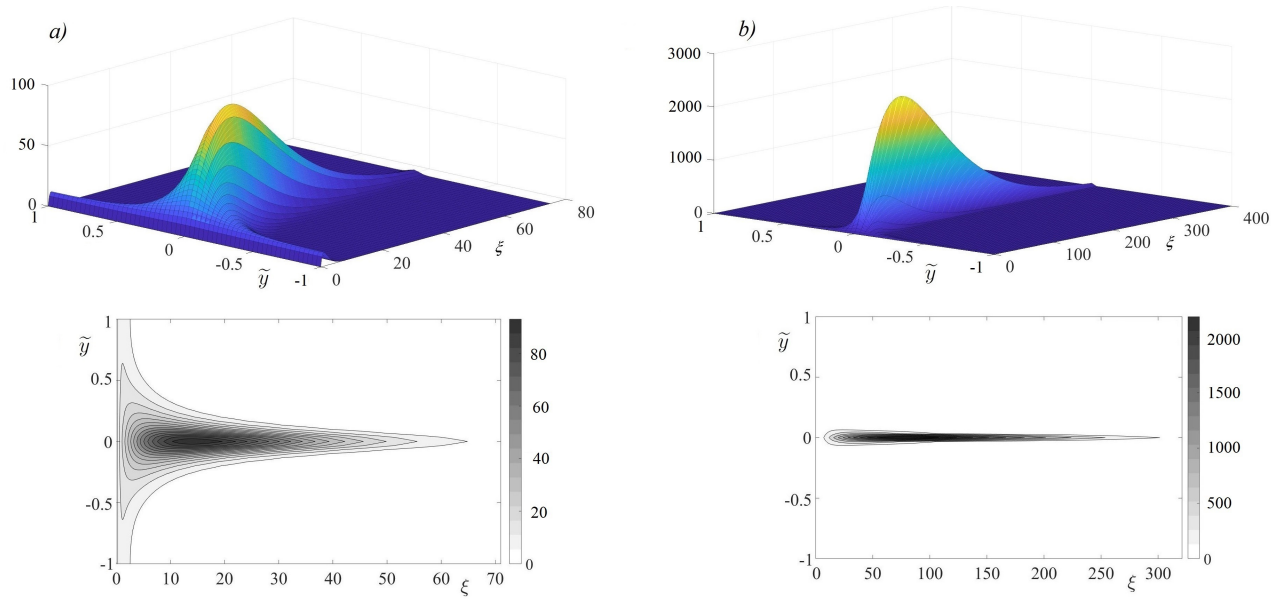

Рис. 3: The forcing term of the ice plate equation (33), $(\widetilde{\varphi}^D_{\widetilde{x}})^F(\xi, \widetilde{y}, 0, 0, \widetilde{z}_0)$, for a dipole moving along the central line of the channel at distance *a)* $|\widetilde{z}_0| = h/2$, and *b)* $|\widetilde{z}_0| = h/10$ from the ice cover in the dimensionless variables.

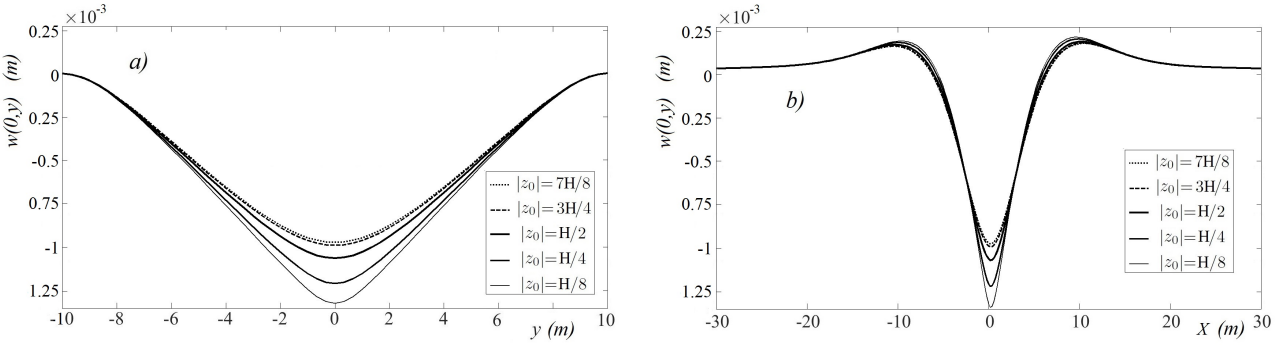

Рис. 4: Deflection of the ice cover *a)* across the channel at $X = 0$, and *b)* along the central line of the channel, $y = 0$. The speed of the dipole is $U = 3$ m/s. Depth $|z_0|$ is shown in the legend, H=2 m.

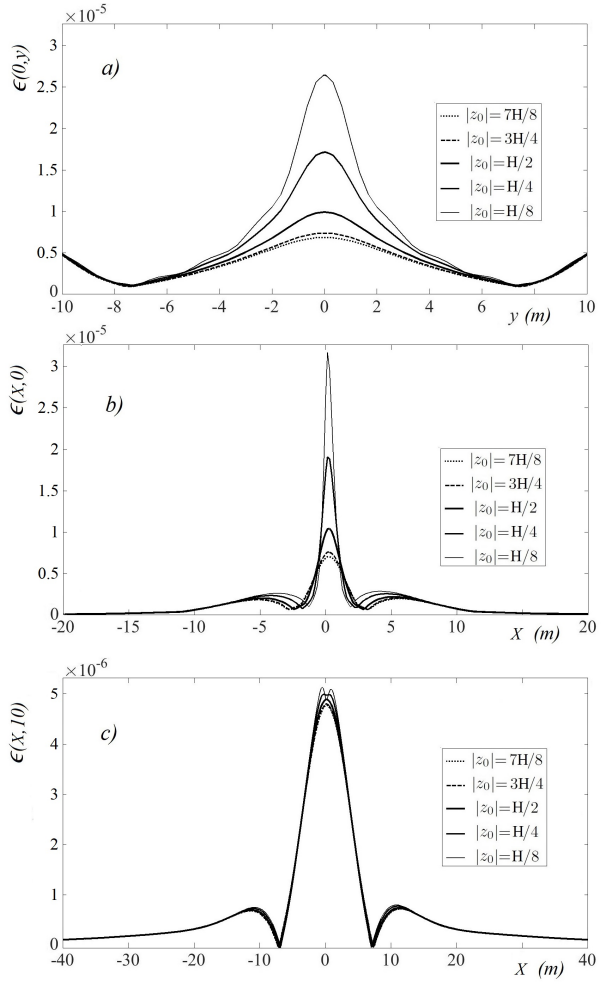

Рис. 5: Strains *a)* across the channel at $X = 0$, *b)* along the central line of the channel, $y = 0$, *c)* along the vertical walls of the channel, $y = \pm 10$ m, for $U = 3$ m/s and $H = 2$ m.

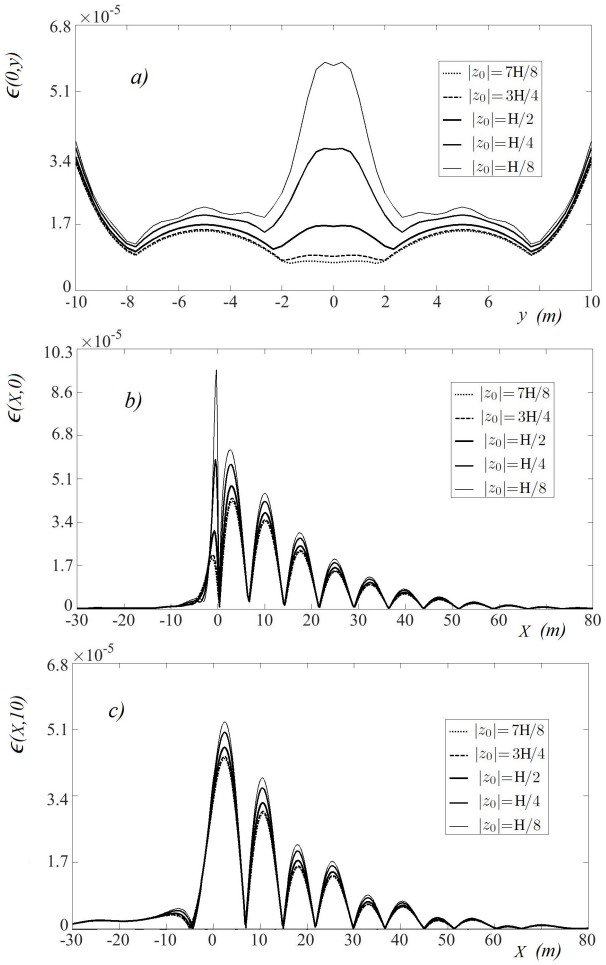

Рис. 6: Strains *a)* across the channel at $X = 0$, *b)* along the central line of the channel, $y = 0$, *c)* along the vertical walls of the channel, $y = \pm 10$ m, for $U = 7$ m/s, $H = 2$ m.

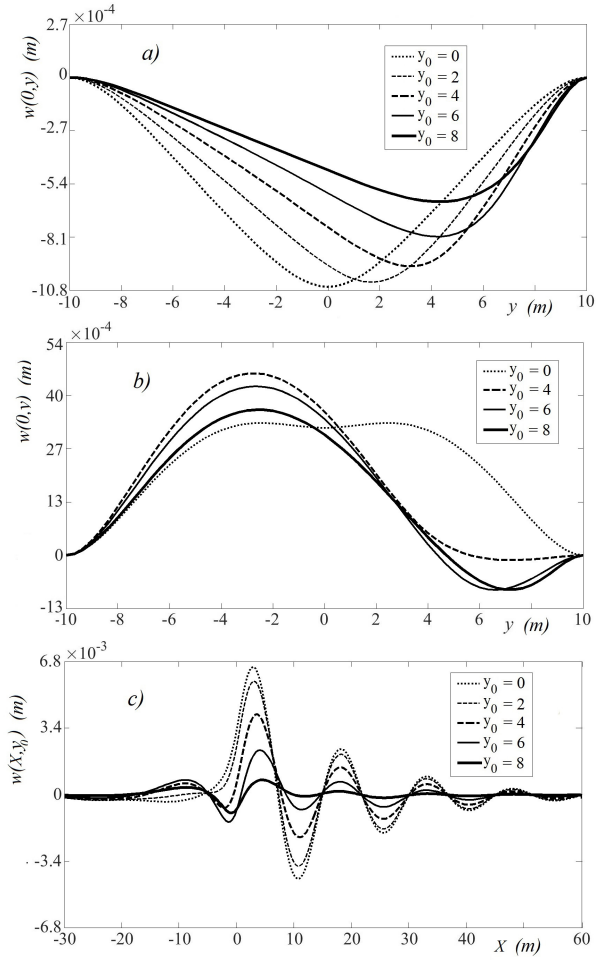

Рис. 7: Deflections of the ice cover across the channel above the dipole, $X = 0$, for the speed of the dipole *a)* $U = 3$m/s, *b)* $U = 7$m/s. *c)* Deflection along the channel above the dipole, $y = y_0$, for the speed 7 m/s. Position of the dipole y_0 is shown in the legend in metres.

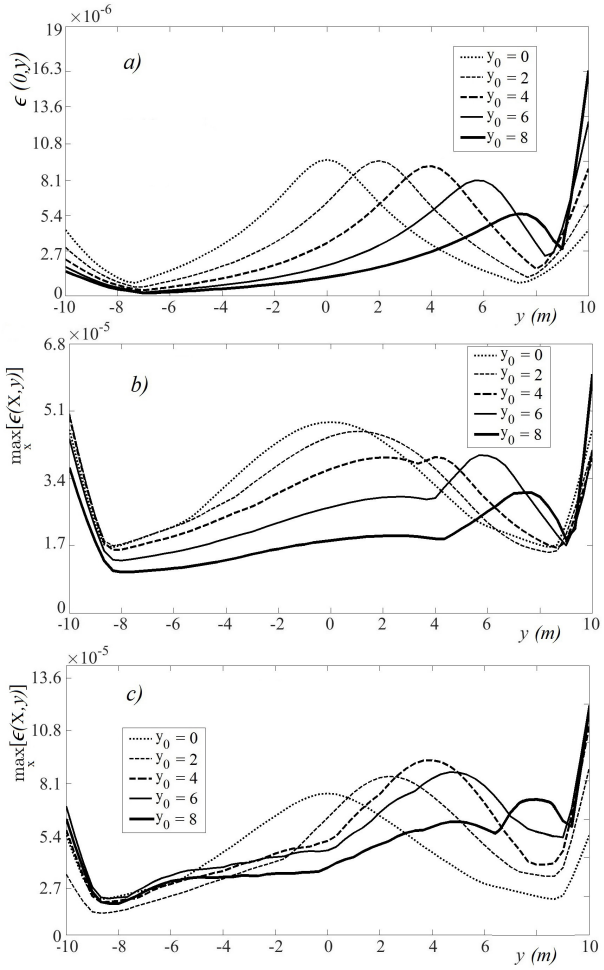

Рис. 8: The strains of the ice cover above the dipole, $X = 0$, for the dipole moving closer to the right wall of the channel *a)* at speed $U = 3$m/s for different y_0. *b)* The maximum strain along the channel as a function of y for the supercritical speed $U = 7$m/s. *c)* The maximum strain along the channel as a function of y for the supercritical speed $U = 12$m/s. The dipole moves at depth $z_0 = 1$ m, y_0 is shown in metres in the legend.

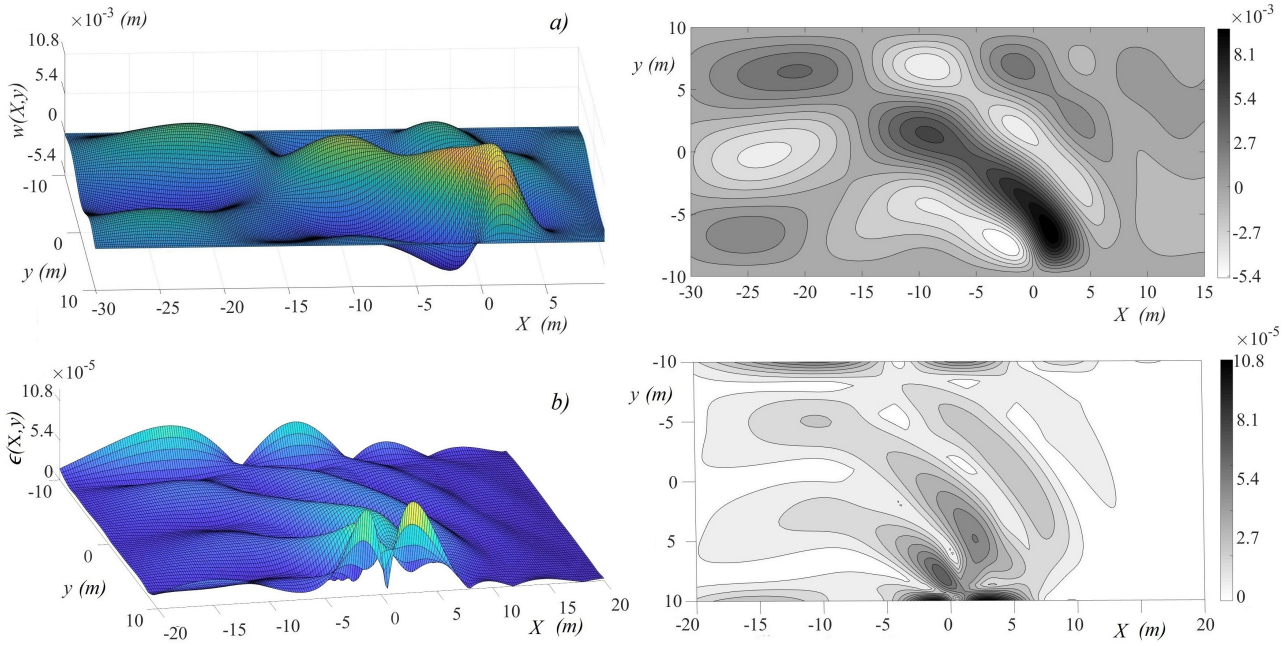

Рис. 9: The ice deflections *(a)* and strains *(b)* as functions of X and y for the dipole moving at speed $U = 12$ m/s at $|z_0| = 1$ m and $y_0 = 8$ m.